

extract was concentrated 20-fold and an aliquot chromatographed on the amino acid analyzer using a stream splitter attachment. Fractions constituting a single, radioactive peak were pooled and individually cochromatographed with authentic samples of the tabtoxins and their hydrolytic products.

Results. Culture filtrates from isolates of *P. tabaci* and *P. coronafaciens*, with the exception of 1 isolate of each species, were capable of hydrolyzing tabtoxins when incubated at 37°C but not 4°C (figure). Addition of diethylpyrocarbonate or adjustment of the pH to 2 or 10 abolished peptidase activity. The 40–70% ammonium sulfate fraction from all the plant species and diseased tobacco also hydrolyzed the tabtoxins. However, preparations of the intercellular fluids from both healthy and diseased tobacco leaf tissues had no detectable activity.

Analysis of gel electrophoretograms of the bacterial and plant preparations showed that hydrolysis was due to multiple enzymes; every section of the gels exhibited activity. When duplicate gel sections were stained with Coomassie brilliant blue, discrete protein bands became visible, indicating that the protein separations were satisfactory. All bacterial and plant preparations having peptidase activity on the tabtoxins were inactive on the isotabtoxins. The same result was obtained with leucine aminopeptidase. Most ($\geq 85\%$) of the radioactivity after incubation of the ^{14}C -tabtoxins in tobacco leaves was still associated with the tabtoxins or their products. It was distributed among these compounds as follows: tabtoxine- β -lactam, threonine and serine, 8.5%; tabtoxins 75%; isotabtoxins 6%; and an unknown compound or compounds, 11%, eluting 11 min after tabtoxine- δ -lactam. A sterile solution of ^{14}C -tabtoxins maintained in buffer, pH 7, at 28°C for 36 h did not have any hydrolysis products when similarly analyzed. The same result was also obtained when ^{14}C -tabtoxins and a tobacco leaf preparation were processed immediately after mixing.

Discussion. Collectively, these results strongly suggest that the tabtoxins are hydrolyzed during disease development. Most likely this occurs in the plant cells, possibly within the vacuole¹⁴, by the action of multiple enzymes having peptidase activity. Hydrolysis of the tabtoxins also could occur in the intercellular spaces by bacterial and/or plant action but no evidence to support this notion was obtained.

Hydrolysis of tabtoxins appears to be of biological significance because our initial experiments have shown that tabtoxine- β -lactam inhibits GS, whereas the tabtoxins do

not. If further detailed work substantiates GS as the primary site of action, it would mean that hydrolysis is a prerequisite for activity. A chlorosis-inducing toxin produced by *P. phaseolicola* (Burkh.) Dowson, phaseolotoxin, has already been reported to be hydrolyzed by plant enzymes; however, phaseolotoxin itself is as active an inhibitor of ornithine carbamyl transferase (OCT) as one of the hydrolytic products, N δ -(phosphosulphamyl) ornithine¹⁵. Thus, it does not appear that in this case hydrolysis is mandatory for biological activity, assuming that OCT is the primary site of action and that the OCT preparation did not hydrolyze phaseolotoxin.

How widespread the occurrence might be of metabolic activation of phytotoxins is currently unknown. However, many are potential candidates having structures containing hydrolyzable bonds or groups that are readily modified^{16,17}. We suggest that the metabolic products of toxins could, if they are also toxic, have different affinities or even different sites of action from the parent compound(s). More emphasis should be given to examining the metabolism of phytotoxins as part of studies on their mechanism of action.

- 1 R.D. Durbin, in: Morphological and Biochemical Events in Plant-Parasite Interaction, p.369, Ed. S. Akai and S. Ouchi publisher, town 1971.
- 2 P.A. Taylor, H.K. Schnoes and R.D. Durbin, Biochem. biophys. Acta 286, 107 (1972).
- 3 W.W. Stewart, Nature 229, 172 (1971).
- 4 A.C. Braun, Phytopathology 45, 659 (1955).
- 5 F. Meins, Jr and M.L. Abrams, Biochem. biophys. Acta 266, 307 (1972).
- 6 A. Meister and S.S. Tate, A. Rev. Biochem. 45, 559 (1976).
- 7 S.L. Sinden and R.D. Durbin, Nature 219, 379 (1968).
- 8 H. Kingdon, J.S. Hubbard and E.R. Stadtman, Biochemistry 7, 2136 (1968).
- 9 R.D. Durbin, T.F. Uchtyl, J.A. Steele and R. Ribeiro, Phytochemistry 17, 147 (1978).
- 10 R.D. Durbin and S.L. Sinden, Phytopathology 57, 1000 (1967).
- 11 D.W. Woolley, G. Schaffner and A.C. Braun, J. biol. Chem. 215, 485 (1955).
- 12 J.L. Rosemont, Analyt. Biochem. 88, 314 (1978).
- 13 Z. Klement, Phytopathology 55, 1033 (1965).
- 14 M. Nishimura and H. Beevers, Nature 277, 412 (1979).
- 15 R.E. Mitchell and R.L. Bielecki, Pl. Physiol. 60, 723 (1977).
- 16 R.P. Schaffer, in: Encyclopedia Plant Physiology, vol. 4, p. 247. Ed. H. Heitefuss and P.H. Williams. Springer, Berlin 1976.
- 17 K. Rudolph, in: Encyclopedia Plant Physiology, vol. 4, p. 270. Ed. H. Heitefuss and P.H. Williams. Springer, Berlin 1976.

Simple, geometrical model for a typical echinocyte III

R. Martino, M. Negri and A. Di Marco

Institute of Human Physiology (1st Chair), Faculty of Medicine, Padua University, via Marzolo, 3, I-35100 Padova (Italy), 23 April 1979

Summary. The purpose of the present work is to obtain information relative to the volume and surface area of echinocyte, type III, on the basis of simple, micrographical evidence. A concrete case has been examined as direct demonstration of theory and techniques of calculus.

It is obvious that it is impossible to know certain geometrical data, as the surface area, relative to any spatial structure (cells, organs or other bodies) without some theoretical information and functional hypotheses, concerning the shape and dimensional ratios of the body in question.

In other words the evaluation of a particular kind of geo-

metrical data implies the adoption of an appropriate model, on the basis of known linear parameters (lengths, diameters, axial ratios, etc.) strictly speaking the only geometrical data, which one may measure, i.e. obtained by means of a direct, empirical determination.

Having stated this, we present a typical situation, for which

the introduction of a suitable geometrical model is absolutely necessary for the evaluation of two important parameters, i.e. the surface area and the volume.

It is clear that the knowledge of the values, relative to the surface area and volume, is generally very important for the interpretation of the mechanical behaviour of the body at issue, besides for its simple, morphological characterization.

We intend to refer to a particular type of the human erythrocyte, namely the echinocyte III (here labelled as E3), according to Bessis¹ classification. E3 is a cell generally spherical, with 30–50 (regularly) spaced spicules.

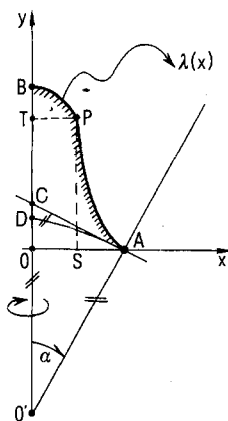
In the present work we give a simple criterion, by means of an appropriate geometrical model, for the evaluation of E3 volume and surface area, on the basis of micrographical evidence.

In order to explain our procedure with the greatest simplicity we limit ourselves to considering a micrograph among the various available. In our analysis, in fact, we refer, without any loss of generality, to a particular scanning electron micrograph, relative to E3 (produced by sodium oleate), obtained by Leblond².

Methods. We introduce 4 hypotheses: a) the central body of the cell is completely spherical, b) the spicules nearly have the same shape and dimensions, c) the spicule axis is on a straight line, containing the centre of the cell body, d) the spicules are regularly spaced.

Volume and surface area of E3 depend on 6 parameters (N , number of spicules; R , spherical cell body radius; H , height of the single spicule; x_f and y_f , inflexional coordinates of the spicule; α , protuberance angle of the spicule), whose values are determinable by means of the micrographic documentation even though with a certain margin of error.

With reference to the figure, we have:



where:

$$\begin{aligned} \overline{OB} &= H & \overline{OO'} &= R \cos \alpha & \overline{O'D} &= \overline{O'A} = R & \overline{OA} &= R \sin \alpha \\ \overline{OS} &= x_f & \overline{OT} &= y_f & P &= \text{inflexion point} \\ \lambda(0) &= H & \lambda(R \sin \alpha) &= d\lambda(x=0)/dx = d^2\lambda(x=x_f)/dx^2 = 0 \\ d\lambda(x=R \sin \alpha)/dx &= -\tan \alpha & \lambda(x_f) &= y_f \end{aligned}$$

It is self-evident that $\lambda(\dots) = \lambda(x=\dots)$ are specifications to the function $\lambda(x)$, visualized in the figure. Moreover:

$$S = 4\pi R^2 + 2\pi N \left\{ \int_0^{R \sin \alpha} x \sqrt{1 + [d\lambda(x)/dx]^2} dx - \int_0^{R \sin \alpha} x \sqrt{1 + [d\mu(x)/dx]^2} dx \right\}$$

with:

$$\lambda(x) = \sum_{j=0}^5 A_j x^j \quad \mu(x) = \sqrt{R^2 - x^2}$$

On the other hand:

$$V = \frac{4}{3} \pi R^3 + 2\pi N \left\{ \int_0^{R \sin \alpha} [\lambda(x) - \mu(x)] dx + \frac{1}{2} R^3 \cos \alpha \sin^2 \alpha \right\}$$

The coefficients A_j ($j=0, 1, \dots, 5$) of $\lambda(x)$ are given from:

$$\begin{aligned} A_0 &= H & A_1 &= 0 & A_2 &= D_2/D & D \text{ and } D_{(1)} &= \text{the determinants, relative to the polynomial collocation system, with } \lambda(x) \text{ on } P, B, A \text{ points} \\ A_3 &= D_3/D & A_4 &= D_4/D & A_5 &= D_5/D \end{aligned}$$

Results. In the particular case, here considered (see figure), we have (approximately):

$$\begin{aligned} R &\simeq 3.6 \mu\text{m}; \\ N &\simeq 36; \\ H &\simeq 1.0 \mu\text{m}; \\ x_f &\simeq 0.3754428 \mu\text{m}; \\ y_f &\simeq 0.6666666 \mu\text{m}; \\ \alpha &\simeq 9^\circ. \end{aligned}$$

The above-mentioned values, relative to characteristic lengths or angles of the E3, must be referred to a single, typical cell, examined by means of appropriate techniques of microscopy.

So that:

$$\begin{aligned} D &= 0.132248 \text{ E} - 04 & \text{exponential notation} \\ D_2 &= 0.539720 \text{ E} - 03 \\ D_3 &= -0.308049 \text{ E} - 02 \\ D_4 &= 0.518930 \text{ E} - 02 \\ D_5 &= -0.275695 \text{ E} - 02 \end{aligned}$$

Finally we obtain, by means of an appropriate (Fortran IV H language) program for the computer:

$$\begin{aligned} S &\simeq 256.9133 \mu\text{m}^2 \\ V &\simeq 216.2730 \mu\text{m}^3 \end{aligned}$$

For the sake of brevity and simplicity we have valued the surface area integral and volume integral not analytically but numerically by means of the Simpson's formula on the basis of an ordinary and very usual subroutine.

Discussion. The numerical results for S and V of the particular cell, here treated as concrete example of application of our formula, may be interpreted from 2 different viewpoints, i.e.: 1. the cell, here considered, represents a case of echinocyte, extraordinarily bulky 'ab origine'; 2. the transition to E3 form implies large surface and volume dilatations. We consider the first hypothesis as the more probable one.

On the other hand these are nothing but simple illations. The only point, here remarkable, is the framework of the system of hypotheses and the choice of functions, by means of which one may deduce from micrographical reports metric and morphological information, otherwise unapproachable.

- 1 M. Bessis, in: Red Cell Shape, p. 1. Springer, New York 1973.
- 2 P. Leblond, in: Red Cell Shape, p. 95. Springer, New York 1973.